On the CO2 Capture in Water-Free Monoethanolamine Solution: An Ab Initio Molecular Dynamics Study.

ARTICLE · APRIL 2013

DOI: 10.1021/jp4022932 · Source: PubMed

4 AUTHORS, INCLUDING:

Bo Han
China University of Geosciences
31 PUBLICATIONS **187** CITATIONS
SEE PROFILE

Maohong Fan
Univ. Wyoming and Georgia Tech
293 PUBLICATIONS **4,232** CITATIONS
SEE PROFILE

Hansong Cheng
China University of Geosciences
166 PUBLICATIONS **2,397** CITATIONS
SEE PROFILE

THE JOURNAL OF PHYSICAL CHEMISTRY B

Article

pubs.acs.org/JPCB

On the CO_2 Capture in Water-Free Monoethanolamine Solution: An ab Initio Molecular Dynamics Study

Bo Han,[†,‡] Yubao Sun,[†] Maohong Fan,[§] and Hansong Cheng*[,†,‡]

[†]Department of Chemistry, National University of Singapore, 3 Science Drive 3, Singapore

[‡]Sustainable Energy Laboratory, China University of Geosciences Wuhan, 388 Lumo RD, Wuhan 430074, China

[§]Department of Chemical and Petroleum Engineering, University of Wyoming, Laramie, Wyoming 82071, United States

Supporting Information

ABSTRACT: Monoethanolamine (MEA) based liquids are widely used materials for postcombustion CO_2 capture. We report here an extensive ab initio molecular dynamic (AIMD) simulation study on CO_2 sorption in water-free MEA liquid with a range of CO_2 contents at 313 K. The simulation reveals the detailed CO_2 capture mechanism that leads to the initial formation of a zwitterion species and the ultimate proton transfer from the zwitterion to a nearby MEA molecule. The ion pairs formed in the liquid result in strong electrostatic interactions among the molecules in the liquid. The variation of liquid density, volume, diffusion coefficient, power spectrum, and average heat of sorption at the selected CO_2 loadings was systematically assessed. The results indicate that initially the volume of the MEA solution expands gradually and tops at 60% of CO_2 loading. After that, the volume declines as a result of strong Coulomb interactions among the ion pairs at higher CO_2 loadings. The calculated liquid densities and the average heats of sorption are in quantitative agreement with the available experimental values. The simulated power spectrum of the water-free liquid also resembles the infrared spectrum of 30% aqueous MEA solution. The characteristic features in the simulated power spectra are slightly blue-shifted upon CO_2 uptake.

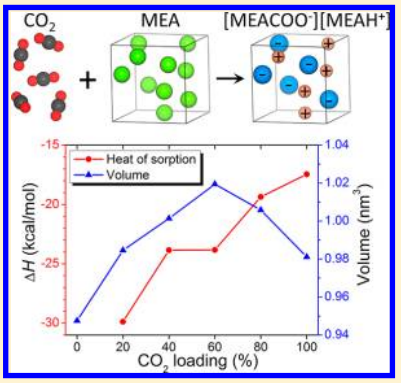

INTRODUCTION

Effective control of the massive CO_2 emission has become an increasingly pressing technological issue and represents one of the grand challenges for sustainable utilization of energy resources.[1,2] CO_2 capture of postcombustion flue gas has been found to be one of the most important means to control the release of the greenhouse gas into the environment.[3−5] The amine based organic liquids and ionic liquids have long been found to be highly effective in reversibly absorbing a considerable amount of CO_2 with favorable kinetics and thermodynamics and are thus well-suited for large scale CO_2 capture as sorbents.[6−9] For example, the 30% aqueous monoethanolamine (MEA) solution has been utilized in an industrial scale to capture CO_2 for many years.[10,11] However, with a solution containing 70% of water with high specific heat capacity and vaporization enthalpy, the CO_2 sorption (at 40 °C) and desorption (at 120 °C) cyclic process with the MEA solution is not energy efficient.[12] Other amine-based solutions suffer from similar energy deficiency issues. Therefore, reducing water content in the aqueous solutions of the sorbents could potentially enhance the overall energy efficiency substantially for the amine based CO_2 separation processes as suggested by several CO_2 separation research teams.[12−16] Obviously, use of pure liquid or water-free MEA for CO_2 sorption with a conventional bubbling reactor is not feasible because of the high viscosity of MEA and, thus, the associated slow mass transfer. To overcome the challenges, Sun et al. loaded pure MEA onto the surface of nanoporous TiO_2 for CO_2 sorption and achieved the sorption capacity of 1.09 mol CO_2/kg sorbent as well as complete CO_2 desorption at the temperatures as low as 80 °C, considerably lower than the desorption temperatures needed for aqueous MEA solutions,[17,18] an indication of significant energy saving with the CO_2 separation process.

CO_2 capture in a 30% MEA aqueous solution has been extensively studied both theoretically and experimentally.[19−29] It was found that a CO_2 molecule can rapidly react with a MEA molecule to form a zwitterion intermediate, which subsequently transfers a proton to a nearby MEA molecule to form a $[MEAH^+][MEACOO^-]$ ion pair. Here, water acts primarily as a spectator. The driving force for the capture of CO_2 arises from the proton transfer from one MEA molecule to another upon CO_2 uptake, which leads to the formation of a stable π-conjugated anionic carbamate structure. The strong CO_2 sorption with the measured average enthalpy of sorption ranging from −19 to −24 kcal/mol[19,20] thus demands a relatively high temperature (well above 100 °C) for CO_2 desorption, which is in sharp contrast to what was observed for CO_2 desorption from the TiO_2 supported water-free MEA.[17,18] Unfortunately, the underlying CO_2 capture mechanism associated with water-free MEA liquid based CO_2

Received: March 6, 2013
Revised: April 26, 2013
Published: April 26, 2013

separation has not been fully understood. The intriguing difference in the CO_2 sorption behavior merits detailed mechanistic studies in order to develop more efficient amine based sorbents for postcombustion CO_2 capture. This study was designed to fill the gap.

COMPUTATIONAL METHOD

The water-free MEA was modeled with a periodic cubic box containing 10 MEA molecules as shown in Figure 1. Initially,

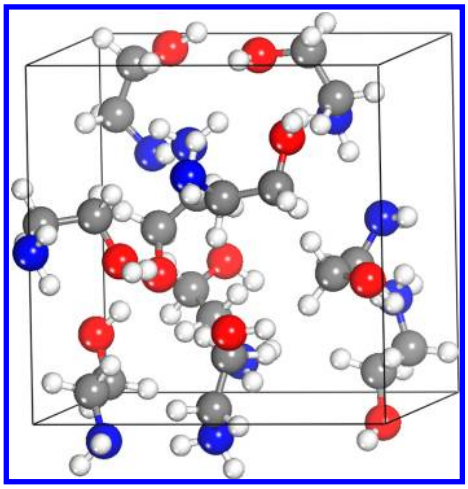

Figure 1. The liquid model of the MEA solution (blue, N; red, O; gray, C; white, H).

the box was built with a slightly larger cell parameter than the corresponding value derived from the experimental density to reserve a certain space for the MEA molecules to reorient upon equilibration. We then performed geometry optimization, with the cell parameter fixed, followed by a 6 ps molecular dynamics (MD) simulation at 313 K to allow the molecules in the box to reorient with stable configurations. Subsequently, full equilibration, including the volume, of the periodic box was performed that yields a cell parameter of 9.914 Å, which gives a liquid density of 1.04 g/cm^3, in good agreement with the experimental value of 1.012 g/cm^3. The same equilibration procedure was utilized to calculate volume variation upon CO_2 uptakes and to derive liquid density at a given CO_2 loading. Subsequently, ab initio molecular dynamics (AIMD) simulations were performed in an NVT-canonical ensemble with the Nosé's thermostat at 313 K (a typical temperature of the flue gas) for over 6 ps[30] with the aim to understand the dynamics of CO_2 capture in water-free pure MEA with various concentrations and the subsequent proton transfer between MEAs upon CO_2 sorption. The physical properties of the sorption systems were then calculated on the basis of the MD simulation results. The power spectrum was derived from the Fourier transform of the velocity autocorrelation function (VAF, $g(t)$) defined by

$$g(t) = \sum_{i=1}^{n} \frac{\langle v_i(t)\cdot v_i(0)\rangle}{\langle v_i(0)\cdot v_i(0)\rangle} \tag{1}$$

where the n is the number of atoms in the system, the v_i is the velocity vector of the atom i, and the angle brackets denote an ensemble average.[31−34] The diffusion coefficients (D) were calculated from the mean square displacement (MSD) using the following equations.

$$\mathrm{MSD} = \langle r^2(t)\rangle = \left\langle \frac{1}{N}\sum_{i=0}^{N} (r_i(t) - r_i(0))^2 \right\rangle \tag{2}$$

$$D = \frac{1}{6}\lim_{t\to\infty}\frac{\mathrm{d}}{\mathrm{d}t}(\mathrm{MSD}) \tag{3}$$

Here, N is the number of particles, t represents time, and $r_i(t) - r_i(0)$ is the vector distance traveled by a given particle over the time interval.

The density functional theory (DFT) calculations were carried out using the PW91 exchange-correlation functional as implemented in the Vienna ab initio simulation package (VASP). The projector augmented wave (PAW) method was used to describe the electron−core interaction, and a planewave basis set was used to describe the valence electrons with a cutoff energy of 430 eV.[35−37] The Brillouin zone integration was sampled with a 2 × 2 × 2 Monkhorst-Pack k point mesh. The nudged-elastic-band (NEB) method[38,39] was utilized to locate the transition states and to evaluate the activation barriers via minimum energy path calculations. The number of images was chosen to achieve smooth curves with a tolerance of 0.003 eV.

RESULTS AND DISCUSSION

To simplify the simulation, only one CO_2 molecule was initially placed in the simulation box containing 10 MEA molecules to understand the details of the sorption dynamics followed by full energy minimization to obtain an optimal box volume and liquid density. The integrity of the CO_2 molecule remains essentially intact upon the structural equilibration. The subsequent AIMD simulation yields numerous molecular configurations in the CO_2 and water-free MEA system. Besides the physical motion of the molecules in the simulation box, similar reaction events observed in CO_2 sorption in 30% aqueous MEA solution also occur during the course of AIMD simulation.

Figure 2a displays the potential energy evolution with simulation time. In the first 2 ps, the CO_2 molecule was found to move rapidly but to retain its molecular integrity. The CO_2 and MEA molecules start reacting after the right molecular orientation emerges. When the C atom of CO_2 is close to the N atom of a MEA molecule in the proximity, a strong covalent C−N bond starts to form leading to the formation of a zwitterion species (MEA^+COO^-) at about 3.6 ps (Figure 3a). The facile zwitterion formation is consistent with the slightly exothermic thermochemical energy of −2.4 kcal/mol and the modest activation barrier of 8.5 kcal/mol obtained upon the minimum energy pathway calculation using the NEB algorithm (Figure 2b). Consequently, the CO_2 molecule is chemically captured. The molecular assembly subsequently undergoes equilibration for an extended duration. After another 12 ps, the assembly still remains physically stable with relatively steady molecular motion. This is different from what has been observed in CO_2 sorption in MEA aqueous solution in which changes of molecular orientation appear to be much faster largely because of the lower viscosity of the liquid. At approximately 16 ps, proton transfer from the zwitterion intermediate to the amine headgroup of a nearby MEA molecule starts to occur via exchange of H atoms with the −OH group of another MEA molecule in between (Figure 3b). Here, the −OH group of the MEA molecule serves as a bridge to facilitate the proton transfer between the zwitterion and the amine headgroup of another nearby MEA molecule. Our NEB

dx.doi.org/10.1021/jp4022932 | J. Phys. Chem. B 2013, 117, 5971−5977

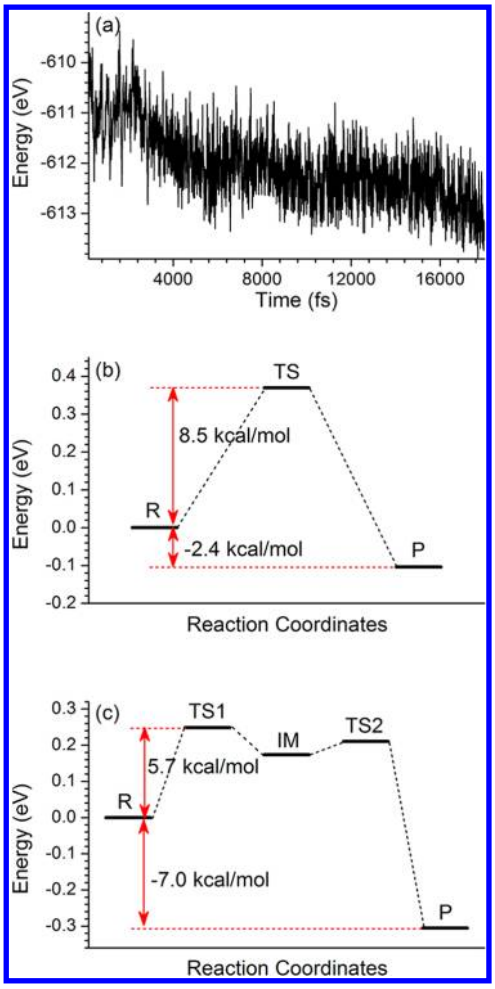

Figure 2. The calculated potential energy profile of (a) the whole MD simulation, (b) the zwitterion formation, and (c) the proton transfer.

calculation on the potential energy profile of proton transfer, shown in Figure 2c, indicates that the reaction is kinetically facile with a moderate activation barrier of 5.7 kcal/mol. A stable ion pair of $MEACOO^-$ and $MEAH^+$ in the liquid is then formed. Alternatively, proton transfer may also occur without being catalyzed by the −OH group if the zwitterion and the targeted amine headgroup are reasonably close (Supporting Information, Figure S1). Indeed, our results from another MD run on the proton-transfer process show that the direct transfer process can occur very quickly with a virtually negligible activation barrier of roughly 1 kcal/mol if both the zwitterion and the amine headgroup are in the proximity of each other, although it requires a higher energy to align the molecules in the orientation that enables the proton transfer.

The proton transfer, driven by the formation of a stable π-conjugated anionic carbamate structure, gives rise to an ion pair of $MEACOO^-$ and $MEAH^+$ in the liquid. Therefore, MEA molecules play a dual role in the CO_2 sorption process. One molecule acts as a CO_2 sorbent and another serves as a proton acceptor reflecting the fact that two MEA molecules are needed to capture one CO_2 molecule. The results indicate that CO_2 capture process in water-free MEA liquid follows essentially the same reaction mechanism as in aqueous MEA solution represented in the following scheme:

$$MEA + CO_2 \leftrightarrow MEA^+COO^- \quad (4)$$

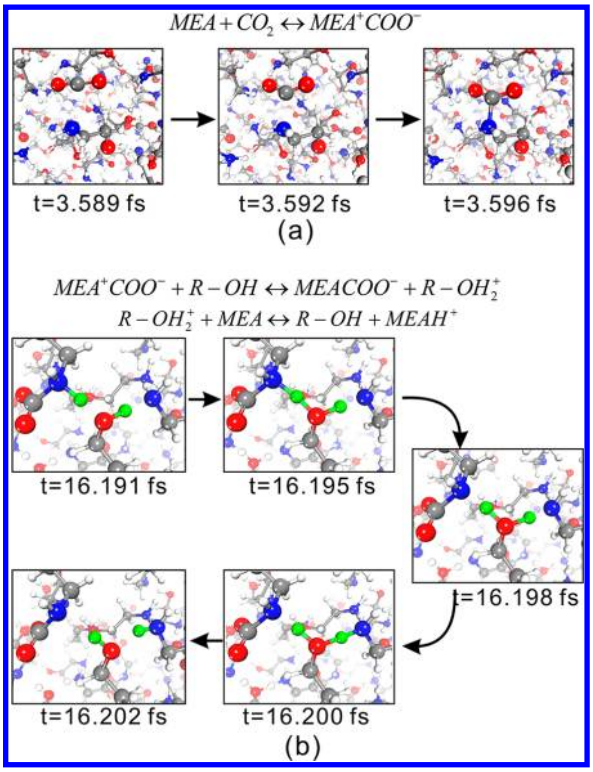

Figure 3. The snapshots of the MD simulation of (a) zwitterion formation and (b) proton transfer. The green balls represent the migrating H atom ($R = NH_2{-}CH_2{-}CH_2$ in the reaction equations).

$$MEA^+COO^- + MEA \leftrightarrow MEACOO^- + MEAH^+ \quad (5)$$

Figure 4a−c displays the calculated radial distribution function (RDF) between the distance of the C atom of CO_2 and the N atom of the MEA molecules for the CO_2 capture process calculated from the MD trajectory in the time intervals of 0−2, 0−4, and 0−6 ps, respectively. The results show that before the first 2 ps (Figure 4a), the C−N distance is more than 3 Å indicating that the CO_2 molecule and the MEA molecules are well separated. A small peak around 1.5 Å then appears in the time interval of 2−4 ps, which is a clear indication of a covalent C−N bond and thus the formation of a zwitterion structure (Figure 4b). The peak continues its strengthening trend with time as the zwitterion is stabilized. Finally, in the time interval of 0−6 ps, the peak intensity at 1.5 Å becomes very pronounced indicating a strong C−N bond in the zwitterion (Figure 4c). Figure 4d displays the calculated diffusion coefficients of the CO_2 molecule in the time intervals of 0−2, 2−4, and 4−6 ps. It shows that the CO_2 molecule initially diffuses in the liquid rapidly until it is captured by a MEA molecule, and then the mobility of the CO_2 molecule diminishes quickly.

On the basis of the reaction mechanism uncovered for the low concentration of CO_2 in water-free MEA, that is, assuming that two MEA molecules capture one CO_2 with formation of ion pairs of $MEACOO^-$ and $MEAH^+$, we performed AIMD simulations sequentially with CO_2 loadings of 20%, 40%, 60%, 80%, and 100% after thorough structural equilibration in each case. Each of the MD runs took approximately 6 ps, and the average energy of the system was calculated over the last 5 ps. The average heat of sorption (ΔH) for CO_2 at a given loading (n) was then evaluated on the basis of the average energies of

dx.doi.org/10.1021/jp4022932 | J. Phys. Chem. B 2013, 117, 5971−5977

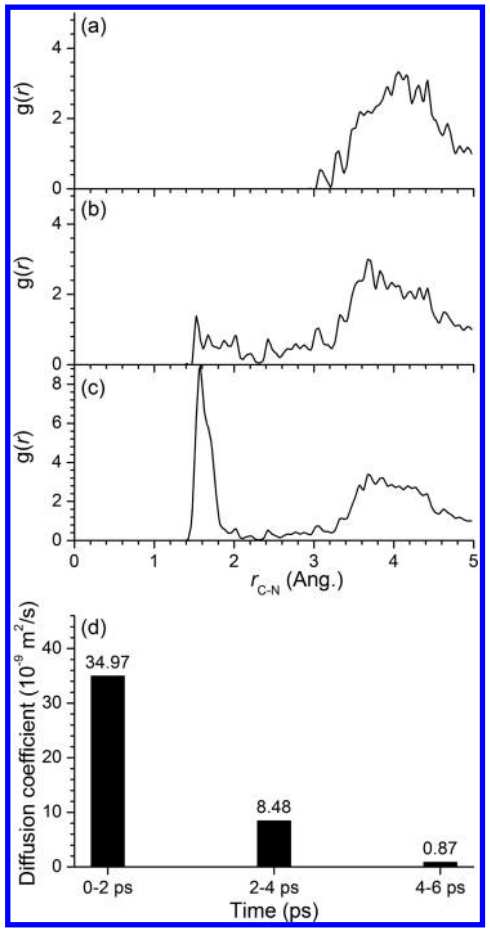

Figure 4. MD simulation results of CO_2 sorption in water-free MEA liquid. The calculated radial distribution function (RDF) between the C atom of CO_2 and the N atom of MEA molecules in the time intervals of (a) 0−2 ps, (b) 0−4 ps, and (c) 0−6 ps. (d) The calculated diffusion coefficient of the CO_2 molecule in the selected time intervals.

the sorption system (E_s), the MEA liquid (E_{MEA}), and the energy of a CO_2 molecule (E_{CO2}) as defined below.

$$\Delta H = (E_s - E_{MEA} - n \cdot E_{CO_2})/n \quad (6)$$

where n is the number of CO_2 molecules in the simulation box. In general, as CO_2 loading in the liquid increases, more ion pairs are formed in the liquid and the solution behaves increasingly like an ionic liquid. With 100% CO_2 loading, the water-free MEA liquid is completely turned into an ionic liquid.

The CO_2 capture and proton-transfer processes reported here bear certain similarities to what has been found in 30% aqueous MEA solution. Specifically, the formation of zwitterion intermediate and the subsequent proton transfer are both facile. However, the water-free MEA liquid exhibits significantly different physical properties as illustrated in Figure 5. Figure 5a describes the variation of liquid volume with CO_2 loading. As the content of CO_2 in the liquid increases, the volume gradually expands and tops at 60%. After that, the volume starts to shrink with CO_2 loading. The volume expansion in the low CO_2 content range is expected as more atoms are added to the liquid. However, the volume shrinkage in the range of high CO_2 loading may be seemingly surprising. The variation can be understood on the basis of the fact that the creation of ion pairs in the liquid gives rise to strong electrostatic interactions, which

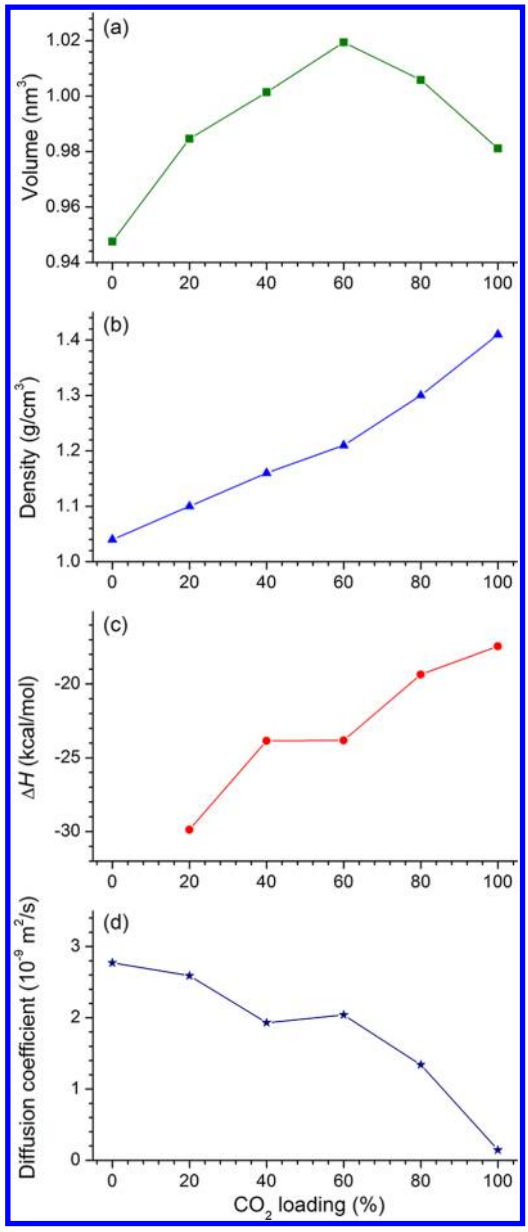

Figure 5. The calculated physicochemical properties of pure MEA solution at various CO_2 loadings. (a) Volume; (b) density; (c) average heat of sorption energy at equilibrium; (d) diffusion coefficient.

allow molecules to be more closely packed. As the amount of the absorbed CO_2 increases, more ion pairs are created and molecular packing becomes increasingly tighter. With 100% CO_2 loading, the solution becomes a pure ionic liquid, and thus, the volume is even lower than the value with 20% loading. In parallel, with the loadings below 60%, the calculated liquid density (ρ), defined by $\rho = W/V$, where W and V represent the total weight and volume of the selected unit cell, increases continuously, and the value rises even further within the higher loading range (Figure 5b). The monotonic rise of liquid density indicates that the mass increase is at a faster rate than the volume expansion and, in particular, when the loadings are higher than 60%, the liquid density increase is further accelerated reflecting the effect of the volume shrinkage.

Weiland et al. proposed a set of empirical equations that correlate solution densities and viscosities with amine composition, CO_2 loading, and temperature for solution-

dx.doi.org/10.1021/jp4022932 | J. Phys. Chem. B 2013, 117, 5971−5977

phase CO_2 capture.[21] According to these equations and their experimental observations, the density and viscosity of aqueous alkanolamine solutions display significant dependence on amine concentration and acid gas loading and were found to increase with CO_2 loading and amine concentration. The recent study conducted by Amundsen et al.[26] on densities and dynamic viscosities in liquid solutions of MEA, water, and CO_2 also indicates a significant increase of density and viscosity at high CO_2 loading (Supporting Information, Figure S2). It was found that the measured densities and viscosities fit very well with the data calculated with the Weiland correlations at a low MEA concentration and CO_2 loading. However, disagreement between the measurements and the Weiland correlations becomes increasingly pronounced as MEA concentration and CO_2 loading increase implying that the Weiland correlations may not be suitable for calculations of liquid density and viscosity for high concentration MEA solutions including water-free MEA. Our simulation results for CO_2 sorption in water-free MEA indicate that the volume shrinkage, caused by the strong electrostatic interactions between ion pairs, is the main reason for the significant discrepancy between the Weiland correlations and the experimental observations by Amundsen et al. At low MEA concentration and CO_2 loading, the concentration of the $MEAH^+$ and $MEACOO^-$ ion pairs is relatively low. Therefore, the ion pairs can be separated easily by water and MEA molecules in the solution to weaken the electrostatic interactions. This gives rise to less volume shrinkage and thus to better agreement between the measurements and the Weiland correlations. However, at high MEA concentrations and CO_2 loadings, strong electrostatic interactions between the ion pairs dominate the molecular packing in the liquid, which prevent the ions from being separated. As a consequence, the Weiland correlations fail to predict the liquid densities and viscosities correctly.

Figure 5c displays the calculated heat of sorption averaged over the course of the MD simulation, excluding the first 1000 steps, versus CO_2 loading. As expected, the average heat of sorption generally decreases with CO_2 uptake. At the full saturation, the calculated average heat of CO_2 sorption or the difference between the activation energy of CO_2 sorption and the activation energy of CO_2 desorption is −17.5 kcal/mol, which is in very good agreement with the experimentally obtained sorption heat of −15.9 kcal/mol. The experimental heat of sorption was calculated with the experimentally derived activation energies of CO_2 sorption and desorption, 3.5 kcal/mol[40] and 19.4 kcal/mol,[18] respectively. The 3.5 kcal/mol was derived with highly concentrated MEA instead of with pure water-free MEA, while the latter was derived with water-free MEA. According to Plaza et al.,[40] the higher the concentration of the MEA, the lower the activation energy of CO_2 sorption is. Therefore, when pure water-free MEA is used, the activation energy of CO_2 sorption should decrease from 3.5 kcal/mol. In other words, the experimentally derived heat of sorption could be very close or equal to −17.5 kcal/mol. Compared to the average heat of sorption in 30% MEA aqueous solution (−22.8 kcal/mol),[29] the value in water-free MEA liquid is considerably lower. This suggests that the temperature needed for CO_2 desorption from water-free MEA can be much lower than that for 30% MEA aqueous solution. Indeed, the recent experimental results indicate that full CO_2 desorption from water-free MEA can be achieved as low as 90 °C,[17] which is substantially lower than the temperatures of spent aqueous MEA regeneration. Furthermore, in particular, the average heat of sorption at 60% CO_2 loading is comparable to the value at 40%. This is attributed to the large volume at 60% uptake, which gives rise to a sufficient space to accommodate the adsorbed CO_2 molecules and thus helps reduce the repulsion between molecules in the system. Finally, the water-free MEA enables essentially all heat to be used for operation of CO_2 capture without spending a large amount of energy to heat up or cool down water, as in the case of aqueous MEA, leading to significantly higher energy efficiency.

From the calculated AIMD trajectories, we evaluated the molecular diffusion coefficients in the liquid on the basis of the mean square displacements. The results are displayed in Figure 5d. Essentially, the calculated diffusion coefficient decreases monotonically as CO_2 loading increases, which is consistent with the increase in liquid density. The calculated diffusion coefficient for pure MEA solution is 2.77×10^{-9} m^2/s, which is in reasonable agreement with the reported experimental value of 1.11×10^{-9} m^2/s for MEA aqueous solution.[41] As the liquid behaves increasingly like an ionic liquid loaded with CO_2, a strong electrostatic interaction becomes a dominant force to dictate molecular motion, which results in closer molecular packing. Consequently, the liquid becomes more viscous, and thus, molecules diffuse much more slowly. Again, the seemingly abnormally high diffusivity at 60% CO_2 loading mainly results from the large volume of the unit cell that benefits the movement of the molecules.

Figure 6 displays the calculated power spectrum of the water-free MEA on the basis of the Fourier transform of the velocity

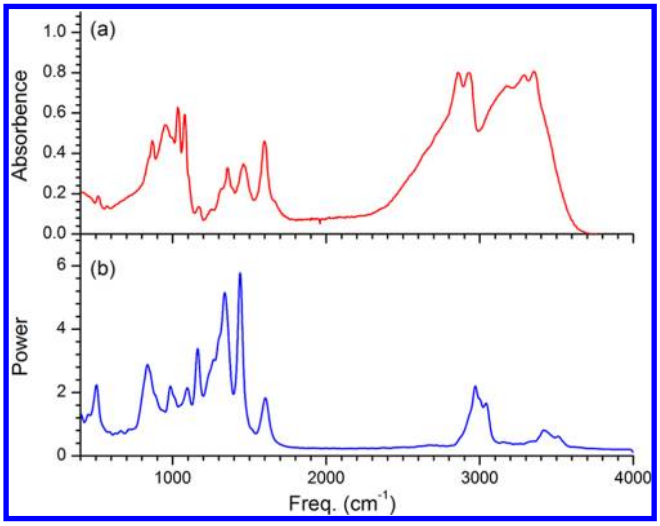

Figure 6. Comparison between (a) the FTIR from experiments and (b) the calculated power spectrum from ab initio MD simulations.

correlation function derived from the MD trajectory.[42] Compared with the experimental Fourier transform infrared (FTIR) spectrum for MEA aqueous solution, the calculated power spectrum reproduces all the basic features displayed in the IR spectrum indicating that the method used in the present work is accurate. The significant broadening observed in the experimental spectrum arises from the large content of water in the MEA solution. Figure 7 describes the effect of CO_2 loading on the simulated power spectra. The results suggest that the characteristic peaks in the spectra are slightly blue-shifted upon CO_2 uptake. Apparently, the vibrational motion of the molecules is increasingly constrained by the gradually enhanced Coulomb interactions between ion pairs. As a result, more

dx.doi.org/10.1021/jp4022932 | J. Phys. Chem. B 2013, 117, 5971−5977

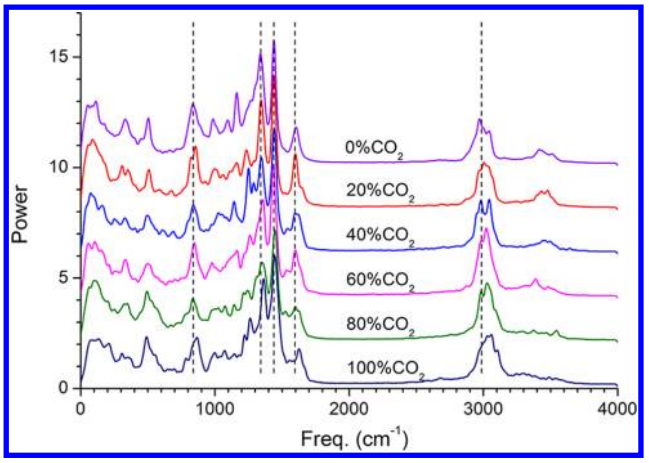

Figure 7. The power spectrum of MEA solution at various CO_2 loadings; the dash lines denote the blue-shifted peaks.

energy is required to move the atoms as featured by the blue-shifted spectra.

CONCLUSIONS

In summary, CO_2 capture in water-free MEA was systematically studied using ab initio molecular dynamics simulations at a typical postcombustion CO_2 separation temperature. It was found that CO_2 sorption in the liquid undergoes a similar reaction mechanism to what was found in aqueous MEA solution. The process is thermodynamically favorable and kinetically facile. The first step of the process is the rapid formation of a zwitterion structure followed by proton transfer from the aminium ion of the zwitterion intermediate to the amine headgroup of a nearby MEA molecule. However, unlike in aqueous MEA, the CO_2 sorption with water-free MEA was found to be significantly less exothermic allowing CO_2 desorption at a substantially lower temperature resulting in a significant decrease in energy consumption for spent MEA regeneration. An additional but important benefit can also be gained by not using water in the sorption process giving a substantial boost of energy efficiency compared to the case in aqueous MEA solution. Our results show that the liquid volume expands gradually to accommodate the CO_2 molecules at CO_2 loadings up to 60%. In contrast, higher CO_2 loadings result in volume shrinkage because of the strong electrostatic interactions between the ion pairs. This gives rise to a faster increase of liquid density of MEA solution at high CO_2 uptake. The calculated diffusion coefficients and power spectra indicate that the movement of the molecular species in the MEA solution becomes difficult upon CO_2 sorption because of the strong Coulomb interaction among ion pairs that dictates molecular interactions. As a consequence, the liquid becomes increasingly viscous as the content of CO_2 increases. The issues associated with the high viscosity can be handled with intelligent engineering design using appropriate support materials. The results of our AIMD simulations yielded the value of the average heats of sorption in excellent agreement with the available experimental data, which demonstrates that the method is capable of quantitatively or semiquantitatively predicting sorption behavior of gases in liquid systems.

ASSOCIATED CONTENT

Supporting Information

The numerical data in Figure 5 are summarized in a table. Figure S1 shows the snapshots of the AIMD simulation during proton transfer. Figure S2 shows the density and viscosity of Amundsen et al.'s results. Figure S3 shows the snapshots of pure MEA solutions with various CO_2 loadings. Table S2 shows the number of molecules/ions used in our calculations. This information is available free of charge via the Internet at http://pubs.acs.org.

AUTHOR INFORMATION

Corresponding Author

*Email: chmch@nus.edu.sg.

Notes

The authors declare no competing financial interest.

ACKNOWLEDGMENTS

We gratefully acknowledge support of the research by a NUS start-up grant, a Singapore National Research Foundation POC grant, and the Singapore-Peking-Oxford Research Enterprise, COY-15-EWI-RCFSA/N197-1. Support from the National Natural Science Foundation of China (Nos. 20873127, 21203169, and 21233006) and the Fundamental Research Funds for the Central Universities, China University of Geosciences, and Wyoming Clean Coal Program in the United States are also gratefully acknowledged.

REFERENCES

(1) Lackner, K. S. A guide to CO_2 sequestration. *Science* **2003**, *300*, 1677−1678.
(2) Rogers, R. D.; Seddon, K. R. Ionic liquids - Solvents of the future? *Science* **2003**, *302*, 792−793.
(3) Kerr, R. A. Global change - No doubt about it, the world is warming. *Science* **2006**, *312*, 825−825.
(4) Kerr, R. A. Global warming is changing the world. *Science* **2007**, *316*, 188−190.
(5) Maginn, E. J. What to Do with CO_2. *J. Phys. Chem. Lett.* **2010**, *1*, 3478−3479.
(6) Metz, B.; Davidson, O.; Coninck, H. d.; Loos, M.; Meyer, L. *Carbon Dioxide Capture and Storage*; Cambridge University Press: Cambridge, U.K., 2005.
(7) Cadena, C.; Anthony, J. L.; Shah, J. K.; Morrow, T. I.; Brennecke, J. F.; Maginn, E. J. Why Is CO_2 So Soluble in Imidazolium-Based Ionic Liquids? *J. Am. Chem. Soc.* **2004**, *126*, 5300−5308.
(8) Gurkan, B.; Goodrich, B. F.; Mindrup, E. M.; Ficke, L. E.; Massel, M.; Seo, S.; Senftle, T. P.; Wu, H.; Glaser, M. F.; Shah, J. K.; Maginn, E. J.; Brennecke, J. F.; Schneider, W. F. Molecular Design of High Capacity, Low Viscosity, Chemically Tunable Ionic Liquids for CO_2 Capture. *J. Phys. Chem. Lett.* **2010**, *1*, 3494−3499.
(9) Gutowski, K. E.; Maginn, E. J. Amine-Functionalized Task-Specific Ionic Liquids: A Mechanistic Explanation for the Dramatic Increase in Viscosity upon Complexation with CO_2 from Molecular Simulation. *J. Am. Chem. Soc.* **2008**, *130*, 14690−14704.
(10) Abu-Zahra, M. R. M.; Schneiders, L. H. J.; Niederer, J. P. M.; Feron, P. H. M.; Versteeg, G. F. CO_2 capture from power plants. Part I. A parametric study of the technical-performance based on monoethanolamine. *Int. J. Greenhouse Control* **2007**, *1*, 37−46.
(11) Feng, B.; Du, M.; Dennis, T. J.; Anthony, K.; Perumal, M. J. Reduction of Energy Requirement of CO_2 Desorption by Adding Acid into CO_2-Loaded Solvent. *Energy Fuels* **2010**, *24*, 213−219.
(12) Tan, J.; Shao, H. W.; Xu, J. H.; Du, L.; Luo, G. S. Mixture Absorption System of Monoethanolamine Triethylene Glycol for CO_2 Capture. *Ind. Eng. Chem. Res.* **2011**, *50*, 3966−3976.

(13) Leites, I. L. Thermodynamics of CO_2 solubility in mixtures monoethanolamine with organic solvents and water and commercial experience of energy saving gas purification technology. *Energy Conv. Manag.* **1998**, *39*, 1665−1674.
(14) Li, J.; Ye, Y. M.; Chen, L. F.; Qi, Z. W. Solubilities of CO_2 in Poly(ethylene glycols) from (303.15 to 333.15) K. *J. Chem. Eng. Data* **2012**, *57*, 610−616.
(15) Bahadori, A.; Vuthaluru, H. B.; Mokhatab, S. Analyzing solubility of acid gas and light alkanes in triethylene glycol. *J. Nat. Gas Chem.* **2008**, *17*, 51−58.
(16) Wu, H.; Chung, T. W. Influences for the addition of ethanol to the absorption system on the interfacial disturbances and mass transfer performance. *Ind. Eng. Chem. Res.* **2008**, *47*, 7397−7404.
(17) Sun, Z.; Fan, M.; Argyle, M. Supported Monoethanolamine for CO_2 Separation. *Ind. Eng. Chem. Res.* **2011**, *50*, 11343−11349.
(18) Sun, Z. Y.; Fan, M. H.; Argyle, M. Desorption Kinetics of the Monoethanolamine/Macroporous TiO_2-Based CO_2 Separation Process. *Energy Fuels* **2011**, *25*, 2988−2996.
(19) Mathonat, C.; Majer, V.; Mather, A. E.; Grolier, J. P. E. Use of flow calorimetry for determining enthalpies of absorption and the solubility of CO_2 in aqueous monoethanolamine solutions. *Ind. Eng. Chem. Res.* **1998**, *37*, 4136−4141.
(20) Kim, I.; Svendsen, H. F. Heat of absorption of carbon dioxide (CO_2) in monoethanolamine (MEA) and 2-(Aminoethyl)-ethanolamine (AEEA) solutions. *Ind. Eng. Chem. Res.* **2007**, *46*, 5803−5809.
(21) Weiland, R. H.; Dingman, J. C.; Cronin, D. B.; Browning, G. J. Density and viscosity of some partially carbonated aqueous alkanolamine solutions and their blends. *J. Chem. Eng. Data* **1998**, *43*, 378−382.
(22) Carson, J. K.; Marsh, K. N.; Mather, A. E. Enthalpy of solution of carbon dioxide in (water + monoethanolamine, or diethanolamine, or *N*-methyldiethanolamine) and (water + monoethanolamine + *N*-methyldiethanolamine) at T = 298.15 K. *J. Chem. Thermodyn.* **2000**, *32*, 1285−1296.
(23) Maham, Y.; Teng, T. T.; Hepler, L. G.; Mather, A. E. Volumetric properties of aqueous solutions of monoethanolamine, mono- and dimethylethanolamines at temperatures from 5 to 80 °C I. *Thermochim. Acta* **2002**, *386*, 111−118.
(24) Ramachandran, N.; Aboudheir, A.; Idem, R.; Tontiwachwuthikul, P. Kinetics of the absorption of CO_2 into mixed aqueous loaded solutions of monoethanolamine and methyldiethanolamine. *Ind. Eng. Chem. Res.* **2006**, *45*, 2608−2616.
(25) Bottinger, W.; Maiwald, M.; Hasse, H. Online NMR spectroscopic study of species distribution in MEA−H_2O−CO_2 and DEA−H_2O−CO_2. *Fluid Phase Equilib.* **2008**, *263*, 131−143.
(26) Amundsen, T. G.; Øi, L. E.; Eimer, D. A. Density and Viscosity of Monoethanolamine + Water + Carbon Dioxide from (25 to 80) °C. *J. Chem. Eng. Data* **2009**, *54*, 3096−3100.
(27) Freguia, S.; Rochelle, G. T. Modeling of CO_2 capture by aqueous monoethanolamine. *AIChE J.* **2003**, *49*, 1676−1686.
(28) da Silva, E. F.; Kuznetsova, T.; Kvamme, B.; Merz, K. M. Molecular dynamics study of ethanolamine as a pure liquid and in aqueous solution. *J. Phys. Chem. B* **2007**, *111*, 3695−3703.
(29) Han, B.; Zhou, C.; Wu, J.; Tempel, D. J.; Cheng, H. Understanding CO_2 Capture Mechanisms in Aqueous Monoethanolamine via First Principles Simulations. *J. Phys. Chem. Lett.* **2011**, *2*, 522−526.
(30) Nose, S. A Molecular Dynamics Method for Simulations in the Canonical Ensemble. *Mol. Phys.* **1984**, *52*, 255−268.
(31) Canto, G.; Ordejon, P.; Cheng, H. S.; Cooper, A. C.; Pez, G. P. First-principles molecular dynamics study of the stretching frequencies of hydrogen molecules in carbon nanotubes. *New J. Phys.* **2003**, *5*, 8.
(32) Kim, J. N.; Yeh, M. L.; Khan, F. S.; Wilkins, J. W. Surface Phonons of the Si(111)-7 × 7 Reconstructed Surface. *Phys. Rev. B* **1995**, *52*, 14709−14718.
(33) Lee, C. Y.; Vanderbilt, D.; Laasonen, K.; Car, R.; Parrinello, M. Ab Initio Studies on the Structural and Dynamic Properties of Ice. *Phys. Rev. B* **1993**, *47*, 4863−4872.
(34) Sankey, O. F.; Niklewski, D. J. Ab Initio Multicenter Tight-Binding Model for Molecular-Dynamics Simulations and Other Applications in Covalent Systems. *Phys. Rev. B* **1989**, *40*, 3979−3995.
(35) Kresse, G.; Furthmuller, J. Efficiency of ab-initio total energy calculations for metals and semiconductors using a plane-wave basis set. *Comput. Mater. Sci.* **1996**, *6*, 15−50.
(36) Kresse, G.; Furthmuller, J. Efficient iterative schemes for ab initio total-energy calculations using a plane-wave basis set. *Phys. Rev. B* **1996**, *54*, 11169−11186.
(37) Kresse, G.; Joubert, D. From ultrasoft pseudopotentials to the projector augmented-wave method. *Phys. Rev. B* **1999**, *59*, 1758−1775.
(38) Henkelman, G.; Jonsson, H. Improved tangent estimate in the nudged elastic band method for finding minimum energy paths and saddle points. *J. Chem. Phys.* **2000**, *113*, 9978−9985.
(39) Henkelman, G.; Uberuaga, B. P.; Jonsson, H. A climbing image nudged elastic band method for finding saddle points and minimum energy paths. *J. Chem. Phys.* **2000**, *113*, 9901−9904.
(40) Plaza, J. M.; Van Wagener, D.; Rochelle, G. T. Modeling CO_2 capture with aqueous monoethanolamine. *Int. J. Greenhouse Control* **2010**, *4*, 161−166.
(41) Ko, C. C.; Chang, W. H.; Li, M. H. Ternary diffusion coefficients of monoethanolamine and *N*-methyldiethanolamine in aqueous solutions. *J. Chin. Inst. Chem. Eng.* **2008**, *39*, 645−651.
(42) Berne, B. J.; Boon, J. P.; Rice, S. A. On the Calculation of Autocorrelation Functions of Dynamical Variables. *J. Chem. Phys.* **1966**, *45*, 1086−1096.